PREDICTION OF PROPAGATION CHARACTERISTICS FOR MICROCELLULAR LAND MOBILE RADIO

Tsukasa IWAMA and Mitsuhiko MIZUNO
Communications Research Laboratory, Ministry of Posts and Telecommunications of Japan
2-1, Nukui-Kitamachi, 4-chome, Koganei-shi, Tokyo, 184, Japan

INTRODUCTION

The use of land mobile radios has been increasing very rapidly. In the mobile communication field, demand for larger capacity communication systems with greater spectral efficiency is increasing more and more. The microcellular system is one of the most promising candidates for this application[1][2]. In order to realize a microcellular system, research of the radio propagation characteristics is a matter of great urgency. In this paper, the use of geometrical techniques for predicting propagation characteristics is described.

Calculations were made using a direct ray and a combination of earth-reflected rays, specular building-reflected rays and building-diffracted rays. Then, to investigate the accuracy of the calculation, predictions were compared with measured values.

THEORETICAL ESTIMATION

The propagation characteristics are determined by interference among the rays to be received at the receiving antenna. In order to determine the propagation path a geometrical ray model which includes the direct ray, specularly reflected rays and diffracted rays is appropriate. These rays are obtained from a building data-base. The rays, which are used in this calculation model, are classified as follows.

1. Direct ray
2. Reflected rays
3. Double reflected rays
4. Diffracted rays
5. Double Diffracted rays
6. Diffracted and reflected rays

The direct ray is calculated from the theoretical free space propagation. Then the field strength E at the receiving dipole antenna is same as theoretical free space field strength E_0.

Reflected rays are calculated from a basic ray model called the plane earth model including some specularly building-reflected rays and earth-reflected rays. This is expanded as follows to calculate the field strength E.

$$E_r = \sum E_0 (d_0/d)\, R \exp(-j\delta) \qquad (1)$$

in which d_0 is the path length of the direct ray, d is the path length of the earth-reflected or building-reflected rays, R is the reflection coefficient of the road or buildings, and δ is the phase difference with respect to the direct ray.

Propagation characteristics are also affected by diffracted and scattered rays. In order to calculate diffracted rays, this model uses the geometrical theory of diffraction(GTD)[3]. For irregular reflections at the wedge, GTD offers several advantages to conventional knife edge diffraction. The field strength of diffracted rays associated with GTD can be expressed as follows;

$$E_d = \sum E^i \cdot \bar{D} \sqrt{\frac{s'}{s(s'+s)}} \exp(-jks) \qquad (2)$$

in which E^i is the electric field incident at the wedge, $\bar{D}$ is the dyadic wedge diffraction coefficient, and s' and s are the distance along the incident ray and diffracted ray. When β_0' and β_0 are the angles respectively between the incident ray and the tangent to the wedge and that between the diffracted ray and the tangent to the wedge,these are equal in GTD, then unit vectors $\hat{\beta}_0'$ and $\hat{\beta}_0$ lie in the plane defined by the wedge and the incident ray and that defined by diffracted ray, respectively. And, when ϕ' and ϕ are the angles respectively between the incident ray and one side plane of the wedge and that between the diffracted ray and same side plane as ϕ', then unit vectors $\hat{\phi}'$ and $\hat{\phi}$ lie in the plane perpendicular to the tangent to the wedge. Thus the dyadic wedge diffraction $\bar{D}$ is described as follows;

$$\bar{D} = \hat{\beta}_0' \hat{\beta}_0 D_s - \hat{\phi}' \hat{\phi} D_h \qquad (3)$$

in which D_s is referred to as the soft scalar diffraction coefficient obtained when the soft boundary condition is used , and D_h is referred to as the hard scalar diffraction coefficient obtained when the soft boundary condition is used.

In the original form of GTD, if the diffracted ray is close to the shadow or reflection boundary, $\bar{D}$ become infinite and discontinuous. This difficulty can be removed by some asymptotic solutions, for example the Uniform Theory of Diffraction(UTD)[4] or Uniform Asymptotic Theory of Diffraction(UAT)[5] and so on. In this paper, UTD method was used.

Field strength of double reflected rays E_{r2} , of double diffracted rays E_{d2} and diffracted and of reflected rays E_{dr} are calculated by a combination of eq.(1) and /or eq.(2).

From these field strengths, the total field strength is calculated as follows;

$$E = E_0 + E_r + E_d + E_{r2} + E_{d2} + E_{dr} \qquad (4)$$

The propagation loss L is defined;

$$L = \frac{p_t g_t g_r}{p_r} \qquad (5)$$

In which p_t is the transmitted power, p_r is the received power, and g_t and g_r are the gain of the transmitting and receiving antenna, respectively. When the receiving antenna is composed of a half-wave dipole antenna, Eq.(5) is expressed as follows;

$$L = \frac{4\pi^2 R_r p_t g_t}{(E \cdot \lambda)^2} \qquad (6)$$

Using Eq.(6), propagation loss may be calculated.

PREDICTION RESULTS

In order to investigate the accuracy of the calculation, predictions were compared with measured values. Measurements were made at 1.480 GHz in the Tokyo metropolitan area[2]. The experiment consisted primarily of mobile measuring vehicle runs along the measured routes, with a fixed transmitting antenna located at the side of the road at height of 5.3 m. Measuring routes and the transmitting point are shown in Fig. 1. Around the measured routes and the transmitting antenna, tall buildings line both sides of the road. In Fig.1, measured route 1 is almost completely located in a line-of-sight propagation environment, while the measured route 2-4 are almost completely shadowed by buildings. The measured routes were full of cars.

In Fig.2, the propagation loss characteristics on measured route 1 are shown. The abscissa represents the distance along the measuring route and the ordinate represents the median of the propagation loss. The 'x' marks show the median of the measured propagation loss. The solid line is

the predicted value from our prediction model. The dotted line shows the point just on side of the transmitting antenna. From Fig.2, the predicted line is very similar to the measured values for almost all points.

Fig.3 and Fig.4 show the comparison result on the measured route 2 and route 4, respectively. The 'x' marks also show the median of the measured propagation loss, and the solid line is the predicted value from our prediction model. The parts between two dotted lines are the intersection with the measured route 1 which is in a line-of-sight propagation environment, other parts are in a shadowed environment. For both figures, near to the intersection, differences between the predicted line and measured values can be seen. This is most probably because of scattering by cars on the measured route 1. In the left parts of the Fig.4, the predicted values became infinite. This is because in our prediction model the number of reflection and diffraction events is limited to 2 and none of these rays reach this region. In order to reduce these prediction errors the number of events must be increased.

Fig.5 shows the prediction errors in a line-of-sight propagation environment. The abscissa represents the distance from the transmitting antenna and the ordinate represents the average of the prediction errors on every 10 m. From Fig.5, most of errors are less than ± 10 dB.

Fig.6 shows the prediction errors in a shadowed propagation environment. The abscissa represents the distance from the intersection with the measured route 1 and the ordinate represents the average of the prediction errors. In Fig.6, except for distances less than 100 m of measured routes 2-4 and for distances greater than 120 m on the measured route 4, almost errors are less than ± 15 dB. In the parts nearer than 100 m, prediction errors are most probably due to scattering by cars on measured route 1. In the part farther than 120 m on the measured route 4, prediction errors are due to the limited number of events.

From Fig.5 and Fig.6, reasonable agreement is obtained in a line-of-sight propagation environment and in a shadowed propagation environment except for regions closer than 100 m to on intersection with a line-of-site road.

CONCLUSIONS

The theoretical estimation using geometrical techniques for predicting propagation characteristics is described. Calculations were made using a direct ray and a combination of earth-reflected rays, specular building-reflected rays and building-diffracted rays.

In order to investigate the accuracy of the calculation, predicted values were compared with measured values. Then reasonable agreement is obtained in a line-of-sight propagation environment and in a shadowed propagation environment except for regions closer than 100 m to on intersection with a line-of-site road.

REFERENCES

[1]S. Kozono and A. Taguchi, "Propagation characteristics of low base-station antenna on the urban road", Trans. IEICE, J72-B-II, pp.34-41, 1989.

[2]T. Iwama, et al., "Investigation of propagation characteristics above 1 GHz for microcellular land mobile radio", Proc. 40th IEEE Veh. Technol. conf., pp. 396-400, 1990.

[3]J. B. Keller, "Geometrical theory of diffraction",J. Opt. Soc. Amer., vol. 52, pp. 116-130, 1962.

[4]R. G. Kouyoumjian and P. H. Pathak, "A uniform geometrical theory of diffraction for an edge in a perfectly conducting surface", Proc. IEEE, vol. 62, pp. 1448-1461, 1974.

[5]S. W. Lee and G. A. Deschamps, "A uniform asymptotic theory of electromagnetic diffraction by a curved wedge", IEEE Trans. Antennas & Propag., AP-24, pp. 25-34, 1976.

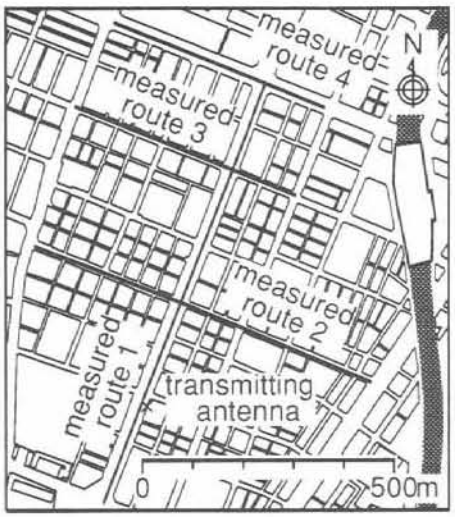

Fig.1 Measured area

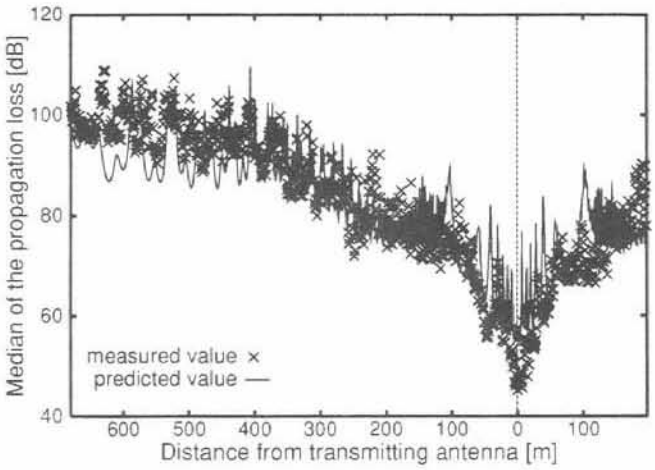

Fig.2 Prediction results in measured route 1

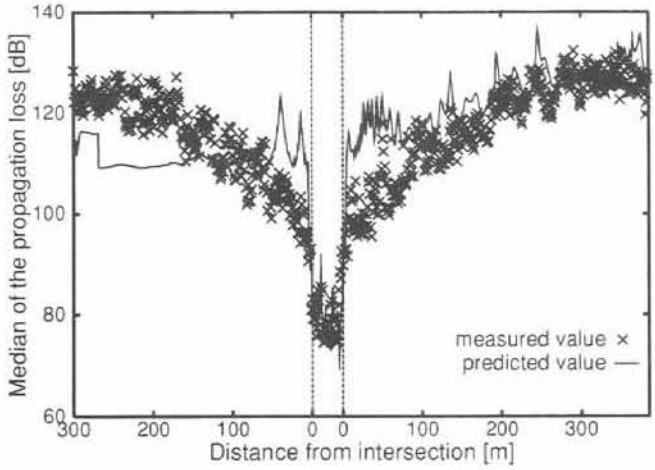

Fig.3 Prediction results in measured route 2

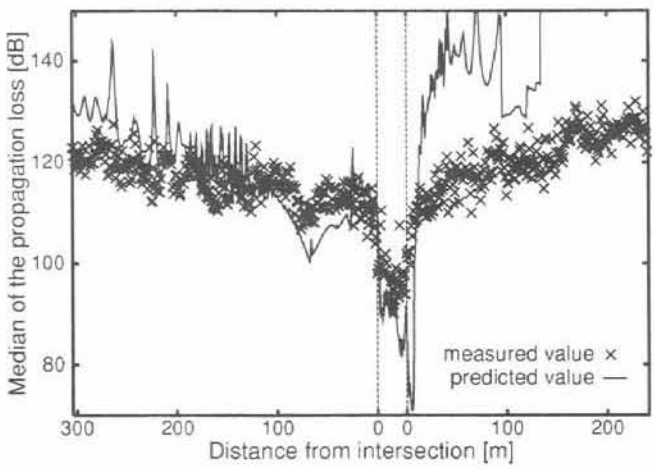

Fig.4 Prediction results in measured route 4

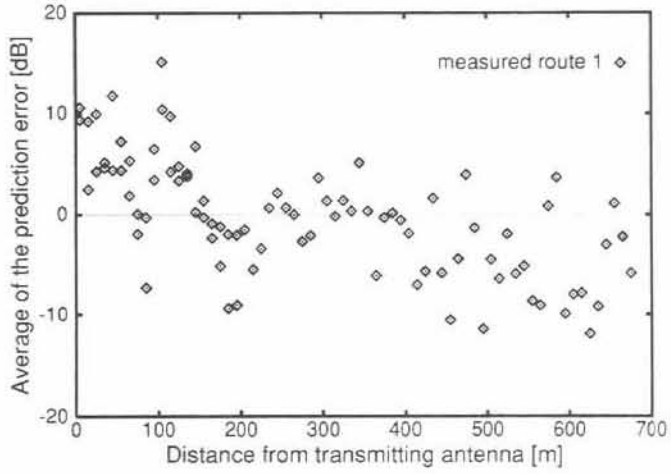

Fig.5 Prediction error in line-of-sight environments

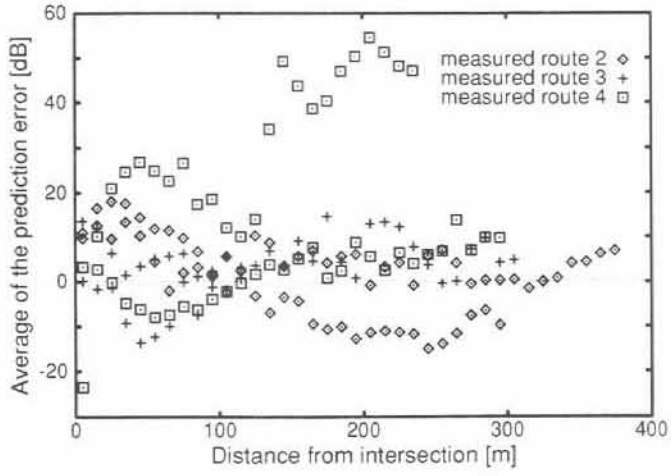

Fig.6 Prediction error in shadowed environments